

Quantum noise limited interferometric measurement of atomic noise: towards spin squeezing on the Cs clock transition

Daniel Oblak, Jens K. Mikkelsen, Wolfgang Tittel,¹ Anton K. Vershovskij,² and Jens L. Sørensen
 QUANTOP, Danish National Research Foundation Centre of Quantum Optics,
 Department of Physics, University of Aarhus, DK-8000 Denmark.

Piotr G. Petrov, Carlos L. Garrido Alzar, and Eugene S. Polzik
 QUANTOP, Danish National Research Foundation Centre of Quantum Optics,
 Niels Bohr Institute for Astronomy, Physics and Geophysics, DK-2100 Copenhagen, Denmark.
 (Dated: 22nd May 2019)

We investigate theoretically and experimentally a nondestructive interferometric measurement of the state population of an ensemble of laser cooled and trapped atoms. This study is a step towards generation of (quasi-) spin squeezing of cold atoms targeted at the improvement of the Cesium clock performance beyond the limit set by the quantum projection noise of atoms. We propose a protocol for the sequence of operations required to generate and utilize spin squeezing for the improved microwave clock performance via a quantum nondemolition measurement (qnd) on the probe light. We calculate the phase shift and the quantum noise of a near resonant optical probe pulse propagating through a cloud of cold ^{133}Cs atoms. We analyze the figure of merit for a qnd measurement of the collective quasi-spin and show that it can be expressed simply as a product of the ensemble optical depth and the probability of the spontaneous emission caused by the off-resonant probe light. In the experimental part we report on the preliminary results on interferometric measurement of the atomic population in a cloud of cold atoms with quantum limited sensitivity.

PACS numbers: 42.50.Lc, 42.50.Nn, 06.30.Ft, 03.65.Ta

I. INTRODUCTION

Quantum noise of atomic magnetization (collective spin) has been first experimentally addressed by Alexандров and Zapassky in [1]. The first observation of the noise with quantum limited, i.e., linear dependence of the variance on the number of atoms was reported in [2]. Later on this quantum limit, called the projection noise limit, has been reached in the state-of-the-art Cs atom clock [3].

Entangled and squeezed state of two ions has been reported in [4]. Spin squeezed state of a cloud of cold Cs atoms in an excited state has been demonstrated in [5]. Qnd measurement was proposed and used to generate a spin squeezed state of atoms in a vapor cell in [6]. Quantum nondemolition measurement with off-resonant light was first proposed as a means for improved clock performance in [6, 7].

In this paper we propose a sequence of spin rotations and qnd measurements which should allow to overcome the projection noise limit for a Cs clock. We describe the theory of a quantum noise limited interferometer with an atom cloud placed in one of its arms. We then proceed to the experiment where we report first results on the in-

terferometric measurement of the atomic population with the sensitivity approaching the quantum limit.

The paper is organized as follows. In theoretical Sec. II we start out with the Bloch sphere picture to illustrate the preparation of and effect of the QND measurement on the coherent state of the caesium atoms. We proceed to derive the equations governing the interaction of the probe field with the caesium atoms, followed by an analysis of the noise contributions to the interferometric signal. The last two theoretical sections deal with the effects creating and counteracting spin squeezing.

In the experimental section we start out with a description and operational properties of the setup with emphasis on the interferometer. We present the results of a measurement of the phase shift due to the atoms in Sec. III D, and in Sec. III E we show the results of a measurement of the atomic noise of our cold atoms. We conclude in Sec. IV and present the outlook towards the future.

II. THEORETICAL DESCRIPTION

A. Pseudo spin in the Bloch sphere representation

Let us first introduce the two level atom formalism to describe our system. Considering a two level atom with the states $|\beta_i\rangle$ (ground) and $|\gamma_i\rangle$ (excited), the density matrix elements are $\hat{\rho}_{ij} = \langle j|\hat{\rho}|i\rangle$ ($i, j = 3, 4$). Note that much of the discussion below does not depend on the magnetic state of the two levels. Such a two level atom

Electronic address: oblik@nb.kd.kz

¹University of Geneva, Group of Applied Physics, 20, Rue de l'Ecole de Médecine, CH-1211 Geneva 4, Switzerland.

²Joint Institute for Nuclear Research, Laboratory of Quantum Magnetometry, St. Petersburg, 194021 Russia.

can be described in terms of a spin one half system with the pseudo spin operators defined by

$$\begin{aligned}\hat{\mathbf{h}}_x^k &= \frac{1}{2} (\hat{\mathbf{h}}_{43}^k + \hat{\mathbf{h}}_{34}^k); \\ \hat{\mathbf{h}}_y^k &= \frac{i}{2} (\hat{\mathbf{h}}_{43}^k - \hat{\mathbf{h}}_{34}^k); \\ \hat{\mathbf{h}}_z^k &= \frac{1}{2} (\hat{\mathbf{h}}_{44}^k - \hat{\mathbf{h}}_{33}^k);\end{aligned}\quad (1)$$

where $\hat{\mathbf{h}}_x^k$, $\hat{\mathbf{h}}_y^k$ and $\hat{\mathbf{h}}_z^k$ are the projection of the angular momentum operator $\hat{\mathbf{h}}^k$ on the x, y and z axes, respectively.

For an ensemble of N_{at} atoms, we define the collective angular momentum operators by $\hat{\mathbf{h}}_x = \sum_k \hat{\mathbf{h}}_x^k$, for the x component, and similarly for the other ones. These operators fulfill the angular momentum algebra $[\hat{\mathbf{h}}_i, \hat{\mathbf{h}}_j] = i\hbar \epsilon_{ijk} \hat{\mathbf{h}}_k$, where ϵ_{ijk} is the Levi-Civita tensor, and are useful for illustrating the evolution of the atomic quantum state using the Bloch sphere representation. This representation is obtained by plotting a vector which x, y and z components are given by the mean values of $\hat{\mathbf{h}}_x$, $\hat{\mathbf{h}}_y$ and $\hat{\mathbf{h}}_z$, respectively. From this picture, the conservation of $\hbar^2 \hat{\mathbf{h}}^2 = \hbar^2 \hat{\mathbf{h}}_x^2 + \hbar^2 \hat{\mathbf{h}}_y^2 + \hbar^2 \hat{\mathbf{h}}_z^2$, which is equivalent to the conservation of the number of atoms, is represented as a trajectory of $\hbar \hat{\mathbf{h}}^2$ on the surface of a sphere. The population difference between the two atomic levels is then given by the projection of $\hat{\mathbf{h}}^2$ on the polar axis ($\hat{\mathbf{h}}_z$), whereas the projection onto the sphere's equatorial plane gives information on the coherent superposition of the two atomic states $|\beta\rangle$ and $|\alpha\rangle$.

In terms of the Bloch sphere representation, our experiment can be viewed as follows: Initially we use optical pumping to prepare the atoms in a coherent spin state with $\hbar \hat{\mathbf{h}}_z \cdot \mathbf{i} = N_{\text{at}}=2$ and $\hbar \hat{\mathbf{h}}_x \cdot \mathbf{i} = \hbar \hat{\mathbf{h}}_y \cdot \mathbf{i} = 0$, as shown in Fig. 1a). In this situation, the atomic variance of $\hat{\mathbf{h}}_x$ is the same as that of $\hat{\mathbf{h}}_y$ and equal to $N_{\text{at}}=4$ [8, 9]. This can be depicted on the Bloch sphere [Fig. 1a)] by an uncertainty disk at the tip of, and perpendicular to the mean value of the angular momentum vector. Since we are interested in reducing the noise of the population difference below the standard quantum limit, for application in atomic clock experiments, we next apply a classical $\pi/2$ pulse using an RF-magnetic field. This pulse brings the angular momentum vector to the equatorial plane as illustrated on Fig. 1b). At this point, we perform the quantum nondemolition (QND) measurement of the population difference $\hat{\mathbf{h}}_z$ using an optical field. This measurement reduces the uncertainty of the operator $\hat{\mathbf{h}}_z$ at the expense of an increased uncertainty of $\hat{\mathbf{h}}_y$ and so, the atomic sample is prepared in a spin squeezed state [Fig. 1e)]. Moreover, the QND measurement will shift the mean value of the pseudo spin vector away from $\hbar \hat{\mathbf{h}}_z \cdot \mathbf{i} = 0$. This deviation will be corrected for by application of a short RF-pulse that will shift the vector back into the equatorial plane of the Bloch sphere [Fig. 1f)]. Since for the caesium clock it is important to have reduced noise during the precession of the phase component $\hat{\mathbf{h}}_y$ in the equatorial plane, we rotate the pseudo spin vector around the y axis with a

$\pi/2$ pulse [Fig. 1g)], which effectively interchanges the $\hat{\mathbf{h}}_y$ and $\hat{\mathbf{h}}_z$ components. The following steps, represented by Figs. 1h) and 1i), correspond to the standard method for Ramsey spectroscopy in the clock operation, but now using a spin squeezed state. If we compare Figs. 1j) and 1k) we clearly see that we gain in signal to noise ratio of the spectroscopy signal from the measurement of the population difference ($\hat{\mathbf{h}}_z$) in the clock transition [10], performed at $(\Delta - \omega_0)T = \pi/2$.

We now draw the attention to the creation of the spin squeezed state in Fig. 1e). It involves the interaction of the atomic ensemble with an optical field that couples the hyperfine ground states to an excited fine structure level.

B. Atomic phase shift

Let us first investigate how an atomic pseudo spin can influence the optical phase of a probe field near resonance. To this end, we start by writing up the complex index of refraction imposed on off-resonant light by a sample of cold multilevel atoms. We consider the alkali D transition $J = 1 \rightarrow J' = 0$ between states having total electronic angular momenta J and J' . The index of refraction is given by [11]

$$n = 1 + \frac{3}{24} \frac{(2J+1)}{2F^2} \left(\frac{N_F (2F'+1)}{F' F} \right)^2 \frac{J_F I}{F' F+1} \frac{1}{\frac{F_F + i}{2} \frac{F_F - i}{2}}; \quad (2)$$

where I and F are the nuclear and total atomic ground state angular momenta respectively, and the primed quantum numbers refer to the excited states. We have also introduced N_F for the atomic density in the level with angular momentum F , $F_F = F_F' + 1$ for the detuning of the probe light from the $F \rightarrow F'$ transition, the atom line width and finally the wavelength, assumed to be common for all transitions making up the considered D line. The Eq. (2) is valid for a polarized probe interacting with a currently experimentally realisable unpolarized atomic ground state so that, the population density in the magnetic sublevel F, m_F of the ground state is $N_{F, m_F} = N_F = (2F+1)$, and we have assumed detunings small enough in order to have $j_{FF'} = 2$, c being the speed of light in vacuum. For the caesium D₂ line ($J = 3/2$) of relevance in our experiment, we have $F = f3;4g$ and $F' = f2;3;4;5g$, as shown on Fig. 2a). Finally, we describe the population of the two hyperfine ground states in terms of the pseudo spin $\hat{\mathbf{h}}_z$.

In the following, we will consider the situation where both hyperfine ground states are close to being equally populated so that, only $\hbar \hat{\mathbf{h}}_z \cdot \mathbf{i} = j$ has nonzero mean value. In the Bloch sphere representation, this situation corresponds to a vector in the equatorial plane as in Fig. 1b).

It is well known [6, 7] that by performing a QND measurement of \hat{J}_z this quantity can acquire a value more well defined than that corresponding to an ensemble of independent atoms and thus spin squeezing of the pseudo spin vector can be achieved.

In our case, the QND measurement is performed by monitoring the optical phase shift of the off-resonant probe interacting with our Cs atoms on the D₂ line. This phase shift is given by $\phi = k_0 l R \text{refn}$ [1g], where l is the physical length of our atomic sample and k_0 is the optical wavenumber. Using the Eq. (2), we find

$$\begin{aligned} & = \frac{1}{2} \left(1 + \frac{N_3}{N} \right) \frac{X^5}{(2F^0 + 1)} \frac{\frac{1}{2} \frac{3}{2} \frac{4}{2} \frac{7}{2}}{F^0 \frac{3}{2} \frac{1}{2} \frac{2}{1}} \frac{4F^0}{4F^0 + 2} \\ & + \left(1 - \frac{N_3}{N} \right) \frac{X^4}{(2F^0 + 1)} \frac{\frac{1}{2} \frac{3}{2} \frac{7}{2}}{F^0 \frac{3}{2} \frac{1}{2}} \frac{3F^0}{3F^0 + 2} ; \quad (3) \end{aligned}$$

where $\phi_0 = \frac{2\pi N}{6}$ and we have introduced the parametrization $N_3 = N(1 - \frac{N_3}{N}) = 2$ and $N_4 = N(1 + \frac{N_3}{N}) = 2$, with N being the overall atomic density and $N = (N_3 + N_4)/N = h\hat{J}_z$.

Using the hyperfine splittings listed in Fig. 2a) and inserting the relevant values for the 6J symbols, we find by solving (3) a zero phase shift of the probe at $\phi_0 = 4312$ MHz relative to the $F = 4 \leftrightarrow F^0 = 5$ transition. At this detuning the phase shifts from the two ground state transitions to the excited state hyperfine manifold cancel for equal populations ($\phi = 0$), as is illustrated in Fig. 2b). Therefore, at ϕ_0 any excursions of ϕ will result in an optical phase shift proportional to ϕ and hence information can be obtained about the collective atomic pseudo spin \hat{J}_z and, in particular, the quantum fluctuations of this observable. Since the latter are the manifestly quantum features of the collective atomic pseudo spin observable, a nondestructive measurement

with the sensitivity at the level of atomic quantum fluctuations will $\propto \hat{J}_z$ to the recorded value at the expense of measurement induced back action noise in the orthogonal \hat{J}_y observable. The state determination will, among other things, be limited by the accuracy of the measurement and hence it is important, for the estimation of the degree of spin squeezing achievable, to evaluate the limiting noise sources of our phase measurement. Also relevant to our study of spin squeezing is the degree to which the probe excites transitions in the atomic medium. Obviously, such excitations will partially cancel the effect of the QND measurement and therefore, it may impose limitations to the achievable degree of spin squeezing.

C. Calculation of the signal-to-noise ratio for the quantum limited interferometry of atoms

For the measurement of the atomic phase shift, we consider the experimental situation illustrated in Fig. 3, where a Mach-Zehnder interferometer is placed around the atomic sample. After the interaction with the atoms the transmission of the interferometer arm is α and the mode overlap at the interference beam splitter is V . The operator corresponding to the input probe field is designated by $\hat{a} = \hat{a}^\dagger + (\hat{x} + i\hat{y})/2$, where \hat{a} is its real mean value and, \hat{x} and \hat{y} are the fluctuating quadrature components. The input photon flux is then $\hat{a}^\dagger \hat{a} = \alpha^2$. Similarly, we introduce the vacuum fields $\hat{b}_k = (\hat{x}_k + i\hat{y}_k)/2$ with $k = 1$ to 4, mixing via the loss processes. At the final beam splitter we must consider two orthogonal spatial modes due to the non perfect mode overlap. Clearly, these modes cannot interfere optically but they will however add coherently in the detector photocurrents. For the photon fluxes impinging on the two detectors we arrive at

$$\hat{a}_1^\dagger \hat{a}_1 = \frac{1}{4} \mathbb{1} + \frac{p}{2} \frac{1}{V} \sin(\gamma) \hat{a}^\dagger \hat{a} + \hat{a}^\dagger \frac{i}{4} \mathbb{1}$$

$$\begin{aligned} & + 2i \frac{p}{V} \sin(\gamma) \hat{b}_1 + \frac{1}{2} \frac{1}{2} \frac{p}{V} e^{i\gamma} (\hat{p} - \hat{b}_2) \\ & + \frac{i}{2} \frac{(1-V)}{2} \hat{b}_3 + \frac{1}{2} \frac{1}{2} \frac{p}{V} e^{i\gamma} \hat{b}_4 + \text{h.c.} ; \quad (4) \end{aligned}$$

$$\hat{a}_2^\dagger \hat{a}_2 = \frac{1}{4} \mathbb{1} + \frac{p}{2} \frac{1}{V} \sin(\gamma) \hat{a}^\dagger \hat{a} + \hat{a}^\dagger \frac{i}{4} \mathbb{1}$$

$$\begin{aligned} & + 2i \frac{p}{V} \sin(\gamma) \hat{b}_1 + \frac{1}{2} \frac{1}{2} \frac{p}{V} e^{i\gamma} (\hat{p} - \hat{b}_2) \\ & + \frac{i}{2} \frac{(1-V)}{2} \hat{b}_3 + \frac{1}{2} \frac{1}{2} \frac{p}{V} e^{i\gamma} \hat{b}_4 + \text{h.c.} ; \quad (5) \end{aligned}$$

where the phase difference $\gamma = 2 \int_{\text{ref}}^R n(L) dL$ is $2 = 2 \int_{\text{probe}}^R n(L) dL$ times the difference of the interferometer arms' optical path length, i.e., the integral

of the index of refraction over the respective arm. From this expression of γ it is clear that the phase can shift because of a change in either the path lengths or the index

of refraction in one of the arm s, or because of a shift of the wavelength of the probe. Moreover, in the probe arm the atom s can change the index of refraction and induce a phaseshift \sim , so that we write $\sim = \sim_0 + \sim_1$ for the total phase shift.

Now, we find the mean photocurrent difference to be

$$\hbar i = \frac{D}{\hat{d}_1^y \hat{d}_1^y} \frac{E}{\hat{d}_2^y \hat{d}_2^y} = \frac{2p}{V} \frac{1}{\cos(\sim)} ; \quad (6)$$

in units of elementary charge. The visibility of our interference fringe is found from the single detector photocurrent and is given by

$$V = \frac{\frac{D}{\hat{d}_1^y \hat{d}_1^y} \frac{E}{\hat{d}_1^y \hat{d}_1^y} \sim_0}{\frac{D}{\hat{d}_1^y \hat{d}_1^y} \frac{E}{\hat{d}_1^y \hat{d}_1^y} \sim_0 + \frac{D}{\hat{d}_1^y \hat{d}_1^y} \frac{E}{\hat{d}_1^y \hat{d}_1^y} \sim_0} = \frac{2p}{1 + \frac{V}{\cos(\sim_0)}} ; \quad (7)$$

In the symmetric case, where $\sim_0 = 1$, this reduces to $V = \frac{p}{V}$ as expected.

The fluctuating part of \sim is now calculated by linearizing around the mean value, $\sim = \sim_0 + \hbar i$, and remembering that only \hat{a} has nonzero mean. As a result we find

$$\begin{aligned} \frac{\sim}{\sim_0} &= \frac{p}{V} \frac{1}{\cos(\sim_0)} [\cos(\sim_0) \hat{x} + \sin(\sim_0) \hat{y}_1] \\ &= \frac{r}{2} \frac{(1 - V)}{V} \hat{y}_3 + \frac{r}{2} \frac{1 - V}{V} [\cos(\sim_0) \hat{x}_4 + \sin(\sim_0) \hat{y}_4] ; \end{aligned} \quad (8)$$

All the field operators in (8) are uncorrelated and consequently for a coherent state input all operators contribute with $2B$, where B is the bandwidth of our measurement [12]. Consequently, we find $(\hat{i})_{coh}^2 = B^2(1 + \sim_0)$, which is just $2B$ times the total photon flux, transmitted through the interferometer.

Let's assume that there are no atoms in the probe arm so that $\sim_0 = 0$. To be sensitive to small phase shifts, we use a second laser far away from the atomic resonance to lock the interferometer at the side of the interference fringe. With this procedure applied to the system, we set the residual phase equal to $(1=2 + m)$ with $m = 0, 1, \dots$; which has the following consequences: Even if our input state is not coherent, or in other words, we are probing the atoms using a noisy laser, we will find the amplitude noise of the probe laser [the first term in (8)] to be considerably suppressed due to the balanced detection. However, the laser phase noise will remain important. We model this noise as an excess noise of the vacuum inputs \hat{x}_1 and \hat{y}_2 , interfering with the probe and contributing with a variance $(1 + N)$ relative to the vacuum state noise while \hat{y}_3 , \hat{x}_4 and \hat{y}_4 still are at the vacuum noise level.

Considering now the presence of atoms, their contribution to the phase noise is denoted $(\sim)^2$, which like the laser phase noise is normalized to the probe vacuum noise level. Incorporating these values into (8) and taking into account the transmission of the interferometer,

we arrive at

$$\frac{(\hat{i})^2}{(\hat{i})_{coh}^2} = 2B + V \frac{N}{N} + \frac{1}{1 + \frac{V}{\cos^2(\sim)}} (\frac{1}{2} \frac{1 - V}{V} \cos^2(\sim)) ; \quad (9)$$

again in units of quantum noise of the transmitted probe and for the case $\sim = (1=2 + m) + \sim_0$.

The excess noise N can be suppressed by operating the interferometer in the white light position since

$$N = \frac{!^2}{(\!^2)_q} (k_0 L)^2 ; \quad (10)$$

where L is the optical path difference between the two arms of the interferometer, $!^2$ is the laser frequency noise and $(\!^2)_q = !_0^2 = \frac{1}{2}$ is the quantum level of frequency noise.

We can also straightforwardly generalize Eq. (9) to detectors with less than unity quantum efficiency, η . In this case we get

$$\frac{(\hat{i})^2}{(\hat{i})_{coh}^2} = 2B + V \frac{N}{N} + \frac{1}{1 + \frac{V}{\cos^2(\sim)}} (\frac{1}{2} \frac{1 - V}{V} \cos^2(\sim)) ; \quad (11)$$

Having addressed the optical noise contributions we will now turn to consider the atomic imprint on the probe phase noise.

D . Spin squeezing

In the context of spin squeezing a high ratio of atom ic spin noise to optical quantum noise is desired. Intuitively this is clear because a higher signal to noise yields more knowledge of the atom ic spin observable, hence it becomes better defined and higher degree of squeezing of that observable is achieved.

Assuming that we have a white light interferometer, the noise contributions of relevance here are the quantum fluctuations (i_p^2) of the phase of the probe pulse and the electronic noise (i_e^2) of our photodetectors. The probe pulse is characterized by the duration τ and the photon number N . Since a highly coherent laser is being used to generate the pulse, we assume it to be Fourier limited [12], $2B\tau = 1$, and then

$$(i_p^2) = 2B\frac{\tau^2}{2} = \frac{\tau^2}{2}; \quad (12)$$

where we have used the photon flux detected from the probe arm $\tau=2$ as reference for the shot noise level.

The electronic noise can be described by the noise equivalent power (NEP), P_e , so that

$$(i_e^2) = (P_e = hc)^2 = 2; \quad (13)$$

h being Planck's constant.

If we ignore the electronic noise [$(i_e^2) = (i_p^2)$] that is only relevant when feedback schemes are involved, we find that the signal to noise ratio of our measurement is given by

$$= \frac{2}{(1 + \frac{\tau^2}{2})^2} = (\frac{\tau^2}{2})^2 \cos^2(\frac{\tau}{2}); \quad (14)$$

which is related to the degree of spin squeezing, as we will see later.

The atom ic contribution to the phase noise is computed from Eq. (3). We assume that the atoms initially are prepared in a coherent spin state for which $(i_{coh}^2) = h\frac{\tau^2}{2}i_{coh} = j^2 = N_{at}^{-1}$, where N_{at} is the number of atoms within the probe volume. Hence, we find that

$$(\frac{\tau^2}{2})^2 = \frac{2D(\frac{\tau}{2})^2}{6A} N_{at}; \quad (15)$$

where A is the probe beam cross sectional area found from the probe beam waist w_0 as $w_0^2=2$ and we have defined the detuning function

$$D(\frac{\tau}{2}) = \frac{x^5}{(2F^0+1)} \frac{(\frac{1}{2}, \frac{4}{2}, \frac{7}{2})^2}{F^0 \frac{3}{2}, 1} \frac{4F^0}{2F^0 + 2} \\ \frac{x^4}{(2F^0+1)} \frac{(\frac{1}{2}, \frac{3}{2}, \frac{7}{2})^2}{F^0 \frac{3}{2}, 1} \frac{3F^0}{3F^0 + 2}; \quad (16)$$

Finally, we find the ratio of the phase noise from the atoms to the quantum phase noise to be

$$= \frac{2D(\frac{\tau}{2})^2}{6A} \frac{2}{(1 + \frac{\tau^2}{2})^2} \frac{VN_{at}}{\cos^2(\frac{\tau}{2})}; \quad (17)$$

For our pulsed measurement we integrate τ over the pulse duration and analyze the statistics of collections of pulses. This sets an upper limit to the frequency of the fluctuations, that we can observe of approximately $\frac{1}{\tau}$. The lower limit is simply set by the time over which we collect the integrated pulses. Since the atom ic noise spectrum is not white, we stress that (17) is only valid to the extent that we match our pulse spectrum to cover the atom ic noise spectrum.

With respect to the spin squeezing, we will be using the following definition taken from [10]

$$= (\frac{\tau^2}{2}N_{at} = h\frac{\tau^2}{2}i_{coh} = j^2); \quad (18)$$

where $= 1$ for a coherent state, < 1 for a squeezed state and $= 1$ for a thermal state. This is not the only way to define the spin squeezing parameter, but this definition characterizes the usability of the state in a spectroscopic measurement, i.e., it is a measure for the increased sensitivity to rotation in the squeezed direction on the Bloch sphere [10].

The degree of spin squeezing can be shown [13, 14] to be related to through

$$= \frac{1}{1 + \frac{\tau^2}{2}}; \quad (19)$$

and thus, the squeezing imprinted by the measurement onto the z-component of the spin is

$$(\frac{\tau^2}{2})_{sq} = (\frac{\tau^2}{2})_{coh} = \frac{1}{4} \frac{N_{at}}{1 + \frac{\tau^2}{2}}; \quad (20)$$

so that, in order to perform a good QND measurement and hence, to achieve a high degree of spin squeezing, we must have > 1 compared to unity. It is natural therefore to call the figure of merit of the qnd interaction. Below we show how τ can be expressed via easily accessible experimental parameters.

So far, we have ignored the electronic noise in the above calculations. It is however important if feedback schemes should be applied in order to either enhance the spin squeezing [15], or if we wish, to rotate the mean spin direction according to our measurement with the goal of obtaining a specific spin squeezed state. The latter is relevant if the spin state should be employed in, e.g., atom ic clocks, where the a Bloch vector in the equatorial plane is desired [16].

The degree of spin squeezing can be measured experimentally by sending pairs of probe pulses through the atom ic sample, integrating these pulse and storing the resulting areas, a_1 and a_2 . The variances $\sigma_1^2 = \sigma_2^2$ will set the level of the atom ic quantum noise, while the variance of the pulse difference $(a_1 - a_2)^2$ will yield information of interatomic correlations created by the quantum

measurement of the first pulse [17]. If we have created a spin squeezed ensemble it will reveal itself via the reduced variance

$$(a_1 - a_2)^2 < a_1^2 + a_2^2 = 2 a_1^2 = 2 a_2^2 : \quad (21)$$

The quantum nature of the atom ic fluctuations can be verified by showing that a_1^2 and a_2^2 are equal and grow linearly with N_{at} .

E. The relation between the gure-of-m erit and atom ic decoherence

The effect counteracting the spin squeezing is the incoherent transfer of atoms from the spin squeezed state via optical excitation to an unpolarized state. This excitation happens with a probability p_e

$$p_e = \frac{(\lambda)}{A} ; \quad (22)$$

where the absorption cross section for the probe is $(\lambda) = (\lambda^2 = 3) L(\lambda)$ with the linewidth function given as

$$L(\lambda) = \frac{X^5}{(2F^0 + 1)} \frac{\left(\frac{1}{2}, \frac{4}{2}, \frac{7}{2}\right)_2}{F^0 \frac{3}{2}, 1} \frac{2}{3F^0 + 2} + \frac{X^4}{(2F^0 + 1)} \frac{\left(\frac{1}{2}, \frac{3}{2}, \frac{7}{2}\right)_2}{F^0 \frac{3}{2}, 1} \frac{2}{4F^0 + 2} : \quad (23)$$

The above cross section assumes both ground states having equal populations and we find that the excitation probability is related to through

$$= V \frac{\lambda^2 D(\lambda)^2}{(1 + \lambda^2)^2} \frac{6A}{L(\lambda)} \cos^2(\phi) N_{\text{at}} p_e : \quad (24)$$

To highlight the relevant physical parameters this equation can be cast into a compact form. If we assume the visibility V , quantum efficiency as well as the transmission of the interferometer all equal to 1, then in the limit of large detunings we have $D(\lambda)^2 = L(\lambda) - 1$ and the DC phase shift becomes negligible so that also $\cos(\phi) = 1$, and Eq. 24 simplifies to

$$= \frac{1}{4} \eta p_e ; \quad (25)$$

where we have introduced η , the atom ic optical depth on resonance. It is clear that, in order to achieve strong spin squeezing we need a large η since we wish to keep p_e small to maintain the non demolishing character of the measurement.

Following the excitation the atoms decay spontaneously to a spherical spin state, i.e., a state characterized by zero expectation value of all spin components $\hbar \dot{\alpha}_i = 0$ ($i = x, y, z$). A detailed analysis of the spin state resulting from the QND measurement and a certain amount of excitation is not straightforward and will be pursued in a future work.

III. SPIN NOISE MEASUREMENTS

A. Magneto-optical trap

The atomic sample is prepared in a standard six beam Cs magneto-optical trap (MOT). We are able to trap around 3×10^8 atoms, when loading the MOT from background Cs vapor with sufficiently high partial pressure (around 10^7 mbar). The red detuning is set to 15 MHz. The cloud volume is approximately 6×10^3 cm³, which at best can yield an optical depth of 15. Due to high background pressure the lifetime of the trap is only around 20 ms. This low lifetime is convenient for acquiring statistical data because it allows for quick refreshing of the atom ic sample.

B. Frequency locking of the probe laser

The probe laser is locked and blue detuned from the atom ic transition $6S_{1/2}(F = 4) \rightarrow 6P_{3/2}(F^0 = 5)$ by a specific detuning variable from a few MHz to a few GHz. The experimental setup used to lock the probe laser in this way is shown in Fig. 4.

Two lasers with a specific relative frequency separation can be locked in a number of ways [18, 19]. We use a reference laser locked to the atom ic transition $6S_{1/2}(F = 4) \rightarrow 6P_{3/2}(F^0 = 5)$ by FM saturation spectroscopy. The reference and a fraction of the probe laser beams are mixed at the beam splitter BS and their beat note is measured using a Newport fast photodetector (model 1480) with 15 GHz bandwidth. The produced RF signal has a frequency component corresponding to the probe detuning from the above specified atom ic transition. This signal is monitored with the spectrum analyzer SA, as shown in the figure. From the RF signal obtained in such a way, we can generate an error signal to lock the probe laser with the desired detuning from the atom ic transition. To accomplish that, the current of this laser is FM modulated using a 1 MHz sinusoidal waveform that is also utilized as a local oscillator for the double balanced mixer DBM in Fig. 4. The output from the mixer is a DC signal that is low pass filtered and amplified before feeding it back to the probe laser controller.

C. White light interferometer

The interferometer as shown on Fig. 5 is a Mach-Zehnder type made of single mode optical fibers. The motivation for using fibers instead of free space propagating beams is the enhanced mechanical stability as well as excellent mode overlap of the interfering beams in single mode fibers. The field in the input fiber enters a 50/50 coupler C1 and is split into a reference arm and a probe arm surrounding the atoms to be probed. The field in the probe arm exits the fiber and with the lens L1 it is focused at the center of the MOT with a beam

waist of 20 m. After passing through the atoms, it again enters the fiber and is combined with the field from the reference arm at the second 50/50 coupler C 2.

Since we use a non-polarization maintaining fiber, the field polarization can evolve differently in the two arms. Thus, in order to achieve maximal interference visibility, we include polarization controllers PC to match the field polarization from the two arms at the second coupler C 2. We note that the coupling efficiency through the air-gap containing the MOT is 30 %. With the fiber couplers providing a nearly perfect mode overlap of the probe and the reference field, i.e., $V \approx 1$, the visibility becomes $V = 85\%$.

The pulsed probe signal is detected with a balanced detection scheme [20] using the low noise photodiodes D 1 and D 2. From the integral of the photocurrent i over the pulse duration, we extract the area which corresponds to the difference of the signals from the two arms. The mean value of the difference gives the DC phase shift ϕ , and the variance gives information about the phase fluctuations.

1. Locking the Interferometer

To reduce thermal and acoustic drifts of the interferometer, we lock it by means of an off-resonant CW laser that propagates through the interferometer simultaneously with, and in the same direction as the probe beam. The locking beam is several nm away from the atomic resonance and therefore it is not affected by the cold atoms. At the output the locking beam and the probe beam are separated by the interference filters F 1 and F 2. The balanced detectors D 3 and D 4 provide an error signal which controls the piezo adjusting the length of the reference arm.

In order to cancel the amplitude noise term in the Eq. (8), the interferometer needs to be locked so that when the cold atoms are absent ($m = 0$) the interference signal for the probe is at half fringe, i.e., $\phi = (1/2 + m)\pi$ with $m = 0, 1, \dots$. However in this position the interference signal is also most sensitive to the phase noise of lasers. We use semiconductor lasers that are characterized by strong phase fluctuations with a wide band of frequencies for both probing and locking. As discussed in Sec. II C, in order to suppress the effect of the phase noise we lock the interferometer at the white light position, corresponding to a nearly zero path length difference [21]. We use a regular broadband LED as a white light source to determine roughly the white light position.

2. Shot noise limited interferometer

To get a measure of the instability or noise of the interferometer signal we measure the variation of the area from one pulse (a_i) to another (a_{i+1}). This is done by

determining the two point variance $\sigma^2(\tau)$ which can be defined to be

$$\sigma^2(\tau) = \frac{1}{2(M-1)} \sum_{i=0}^{M-1} (a_{i+1} - a_i)^2; \quad (26)$$

where τ is the temporal pulse separation and M is the number of pulses in our measurement. The pulse sequences used to compute $\sigma^2(\tau)$ are composed of several thousand pulses each of 2 s duration. From these sequences we can extract the two point variance on time scales comparable with the pulse duration and up to two orders of magnitude in τ . The results corresponding to this measurement are shown in Fig. 6.

If the interferometer noise would be purely white, the two point variance would stay constant on all time scales. Naturally, temperature drifts would cause the variance to rise on larger time scales than those we measure. We observe that the two point variance fluctuates with a period of 200 ms corresponding to 50 Hz line noise. On the scale of Fig. 6, this is seen as a slow rise of the curves. However, on the ms time scale this line noise is of no importance. One interesting feature is seen from the upper trace of Fig. 6. By modulating the laser diode current and thereby, the frequency of the probe laser, we see that $\sigma^2(\tau)$ oscillates with a period corresponding to the modulation frequency. This in turn means that the interferometer is sensitive to frequency changes and therefore, isn't exactly in the white light position. By adjusting the path length difference of the interferometer arms it is possible to come to the white light position and consequently, the oscillation disappears from the two point variance as seen on the lower trace of Fig. 6. This method ensures a fine white light alignment to within 10 m, so that we can have $m = 2$ and fulfill the condition

$\phi = 2\pi m$. Since it is of less concern what is the exact value of m , for the sake of simplicity we assume it to be zero.

It is crucial to find how the interferometer noise, as expressed by the variance of the probe pulses, depends on the power of the probe laser. If the interferometer is shot noise limited, we would expect the noise to scale linearly with the probe power. Applying the same pulse sequence as above described, we first try to determine the noise in the amplitude quadrature. For that purpose, we block the probe arm of the interferometer and just observe the noise of the transmitted beam. In Fig. 7 a fit to the data shows that the amplitude noise depends linearly on the probe power. This shows that our detection is shot noise limited and in addition to that, we have found the shot noise level for later reference.

Next, we unblock the probe arm and look at the phase noise of the interferometer, which in the white light position should be dominated by shot noise. This is also shown in Fig. 7 and one sees that the dependence on the probe power is linear to within the uncertainty of the fit. On this, we conclude that the interferometer is shot

noise limited in the probe power range 0.05 W – 2 W. Moreover, Fig. 7 shows that the quantum noise is similar in the two quadratures, as one would expect from a coherent probe field.

D . Interferometry with cold atoms

We begin with balancing the interferometer at half fringe in the absence of trapped atoms. Trapped atoms cause a DC phase shift of the probe pulse. The measured signal must then be corrected for the absorption of the probe. From the corrected signal i_{DC} , the DC phase shift is deduced as $\phi = \arccos(i_{DC})$. Measuring as a function of the detuning, we observe the dispersive behaviour shown in Fig. 8. Fitting the experimental data points using the Eq. (3), we can determine the density of atoms N

$$N_4 = \frac{C}{21} = \frac{39.9}{(852 \cdot 10^7)^2 \cdot 0.1} = 4.3 \cdot 10^9 \text{ cm}^{-3}; \quad (27)$$

where C is the parameter given by the t and is proportional to ω_0 . This gives an estimated number of atoms probed of $2.2 \cdot 10^5$.

Notice that the theoretical t on Fig. 8 overestimates the amplitude of the $6S_{1=2}(F=4) \rightarrow 6P_{3=2}(F^0=3;4)$ transitions. This can be explained in the following way. We have accounted for the reduction in photon flux and thereby the amplitude of the interference fringes as a result of absorption. However, we did not consider the optical pumping of the atoms due to the absorbed light, and the consequent reduction of the respective atomic density. The reduction of the atomic density at each resonance will depend mainly on the resonant term of the lineshape function $D(\omega)$, where the weight factor of the resonant terms should give the relationship between the absorption probabilities at the three resonances. However, for the $6S_{1=2}(F=4) \rightarrow 6P_{3=2}(F^0=3;4)$ transitions we are pumping atoms over into the $F=3$ ground state, making them insensitive to the probe at the current detuning. On the other hand, the $6S_{1=2}(F=4) \rightarrow 6P_{3=2}(F^0=5)$ transition is a cycling transition since the decay to the $F=3$ ground state is not allowed. Therefore, we do not depump the $F=4$ ground state at this resonance. Consequently, the t to Eq. (3) should avoid points close to the depumped $6S_{1=2}(F=4) \rightarrow 6P_{3=2}(F^0=3;4)$ resonances, and the number C used in Eq. (27) is indeed obtained from such a t .

Closer theoretical calculations that also take stimulated emission and the branching ratios of the excited level decay into account, allow us to determine the time evolution of the level populations for a given detuning and power of the probe. From this the average number of atoms that during the pulse have been pumped over into the $F=3$ ground state can be calculated, and used to estimate the reduction of the DC phase shift due to pumping. With this compensation applied to the data,

the ratios between the amplitudes of the DC phase shift at the three resonances, come very close to values predicted by the transition strengths. We conclude that in the vicinity of the $F=4 \rightarrow F^0=5$ transition the probe does not perturb the atomic population with our measurement conditions.

E . Quantum noise of atomic population

As we can see from Eq. (3), at constant detuning the phase shift is proportional to the density of atoms N . Therefore, given a fixed detuning we can use the DC-phase shift as a measure for the number of atoms probed in the MOT. We vary the number of atoms trapped by varying the background caesium pressure in the chamber.

The optimal choice of the probe detuning is dictated by the balance between the strength of the qnd interaction and the strength of decoherence processes. As in Sec. IID, the signal refers to the photocurrent variance due to atoms and the noise is the photocurrent variance due to other noise sources. Eq. (17) tells us that the signal to noise ratio goes as the square of the detuning function $D(\omega)$ and linearly with the probe flux. From this relationship, we infer that a better signal is obtained at small detunings from the transitions where $D(\omega)$ is large. On the other hand, at small detunings the photon flux would decrease strongly due to absorption by the atoms. Moreover, the excitations can destroy the atomic coherences.

For the data presented here, the spin noise measurements were performed at the detuning of 15 MHz. Using 2 s long pulses of 0.6 W power, this yields a "probability" of atomic transitions of $p_e = 5$. Obviously, this is far from being a QND measurement and the atomic coherence would have been completely lost under such measurement conditions. Normally this would also mean that many atoms are transferred to the $F=3$ ground state, but since we are close to a cycling transition, virtually all of the atoms remain in the $F=4$ ground state after the measurement. Therefore we have effectively relaxed the demand for the measurement to conserve the populations only, but not the coherences. Note that the photon flux is limited only by the detection, which is shot noise limited up to around 1 W.

With this photon flux of $5 \cdot 10^6$, every atom performs about 50 absorption cycles with the probe on resonance, whereby their recoil velocity reaches approximately 1.5 cm/s, which doesn't pose any problems on the timescales of our experiment.

For this measurement we employ a slightly more complex scheme of pulses. Each sequence consists of 3 pulses of a duration of 2 s and equally separated by 10 ms. All three light pulses have the same 0.6 W incident intensity that lies in the range where our detection is shot noise limited. Before each sequence we load the MOT and turn on the magnetic field just before the first of the three pulses. This means that the first pulse 1 probes

the atom ic cloud. With no trapping force to contain it, the MOT has long decayed at the arrival of the second pulse 2. In this way, the pulses 2 and 3 probe the chamber without any atom ic cloud and are used as a reference. We repeat this sequence several thousand times to obtain the statistical information on the pulse areas a_1 , a_2 and a_3 . We subtract the pulse areas pairwise $d_{1,2} = a_1 - a_2$ and $d_{2,3} = a_2 - a_3$, and calculate the mean values $\bar{d}_{1,2}$, $\bar{d}_{2,3}$ and variances $(\bar{d}_{1,2})^2$, $(\bar{d}_{2,3})^2$, over all the recorded sequences.

Now we will address the significance of these variances. For the first pulse the atoms are trapped in the MOT and thus, the pulse area variance $(a_1)^2$ is given by Eq. (11) where, as mentioned earlier, we may neglect the classical phase noise N due to the white light alignment of the interferometer

$$(a_1)^2 = (i_p^2 + 2V^2) \frac{2}{1+} (\phi)^2 \cos^2(\phi) : \quad (28)$$

For the last two pulses, recorded without any cold atoms ($N = 0$), there is no noise term from the atoms and consequently, the variance of the two areas may be written as

$$(a_j)^2 = (i_p^2) ; \quad j = 2, 3 : \quad (29)$$

We see that one ought to be able to extract the shot noise and spin noise from the appropriate pulse areas. What hinders it are slow thermal drifts of the interferometer that would dominate the variance if not corrected for. This is why we subtract the pulses pairwise to cancel the effect of the thermal drifts. Since the shot noise and spin noise are uncorrelated it is easy to verify that for the subtracted areas $d_{1,2}$ and $d_{2,3}$ we have $(d_{1,2})^2 = (a_1)^2 + (a_2)^2$ and $(d_{2,3})^2 = (a_2)^2 + (a_3)^2$ so that we can determine the shot noise and spin noise contributions as

$$(i_p^2) = \frac{(d_{2,3})^2}{2} ;$$

$$(\phi)^2 = \frac{(d_{1,2})^2 - (d_{2,3})^2}{2V^2} \frac{2}{1+} \cos^2(\phi) ; \quad (30)$$

respectively.

In Fig. 9 we show the atom ic contribution to the phase noise $(\phi)^2$ as a function of the DC phase shift ϕ , which, in turn, is proportional to the number of atoms. The linear fit, within the uncertainty, is in agreement with Eq. (15) which predicts the quantum atom ic noise $(\phi)^2$ to scale linearly with N_{at} . The quasi-spin state of our sample in the $F = 3; F = 4$ basis is in a thermal

state, i.e., the mean value of the quasi-spin is zero. However, the quantum noise of such system is equal to the quantum projection noise of the coherent spin state with the same atom ic number which can be, e.g., obtained applying a $\pi/2$ pulse to the $F = 3$ state. Thus the linear scaling shows that we are measuring the population number variance at the quantum projection noise [22].

IV. SUMMARY AND OUTLOOK

In this paper we propose a sequence of qnd measurements and spin rotations which allows to circumvent the projection noise limit of accuracy of the Cs atom clock. The realization of this protocol requires interferometric qnd measurement of the atom ic population with the sensitivity at the projection noise level. Towards this goal we demonstrate experimentally that the shot noise limited fiber optical interferometer at a white light setting can reach this projection noise sensitivity under conditions not far from those of the qnd measurement.

The main parameter that can significantly improve the qnd figure of merit, η , is the optical depth $\frac{2\ln 2}{\delta}$, which is directly proportional to the density of atoms in the probing region. Increasing the optical depth should allow to reduce the photon number and increase the detuning of the probe. Both those measures will improve the spin squeezed state preparation. The atom ic density can be greatly increased compared to our present level by applying a far off resonant trap (FORT), where the dipole force from a focused laser beam traps the cold atoms [23].

Another improvement lies in the optimization of the interferometer, with the aim to reduce losses. This may mean abandoning the fiber interferometer thereby practically eliminating coupling losses ($\eta = 1$). There is another reason why the increased flexibility of a free space interferometer can be an advantage. If the atoms are confined in a dipole trap, the sample will be dense and needle shaped, which will have a lensing effect on the tightly focused probe beam. In this case it is desirable to be able to include compensating lenses into the probe arm. At the present we are working on specifying the properties of the wave directed by atom ic samples with different densities and geometries of the atom ic sample and probe beam.

Acknowledgments

We are grateful to Dr. A. Lvovsky for providing us with the schematics of the detectors used in this work. This research has been supported by the Danish National Research Foundation and by European networks CAUAC and QUICOV.

[1] E. B. A. Aleksandrov and V. S. Zapasskii, Sov. Phys. JETP 54, 64 (1981).

[2] J. L. Sørensen, J. Hald, and E. S. Polzik, Phys. Rev. Lett. 80, 3487 (1998).

[3] G. Santarelli, P. Laurent, P. Lem onde, A. Clairon, A. M ann, S. Chang, A. Luiten, and C. Salomon, Phys. Rev. Lett. 82, 4619 (1999).

[4] Q. A. Turchette, C. S. W ood, B. E. King, C. J. M yatt, D. Leibfried, W . M . Itano, C. M onroe, and D . J. W ineland, Phys. Rev. Lett. 81, 3631 (1998).

[5] J. H ald, J.L. Sorensen, C. Schori, and E.S. Polzik, Phys. Rev. Lett. 83, 1319 (1999).

[6] A. Kuzm ich, N .P. B igelow, and L. M andel, Europhys. Lett. 42, 481 (1998).

[7] A. Kuzm ich, L. M andel, J. Janis, Y .E . Young, R. E jnis man, and N .P. B igelow, Phys. Rev. A 60, 2346 (1999).

[8] J. M . R adcliffe, J. Phys. A 4, 313 (1971).

[9] F. T. A recchi, E. C ourtens, R. G ihm ore, and H .T hom as, Phys. Rev. A 6, 2211 (1972).

[10] D . J. W ineland, J. J. B ollinger, W . M . Itano, and D . J. H einzen, Phys. Rev. A 50, 67 (1994).

[11] I. I. Sobelman, Atom ic spectra and radiative transitions (Springer, Berlin, 1992), 2nd ed.

[12] A .Y ariv, Optical Electronics in M odern C omm unications (Oxford University Press, 1997), 5th ed.

[13] L. M . D uan, J. I. C irac, P. Zoller, and E .S. Polzik, Phys. Rev. Lett. 85, 5643 (2000).

[14] P. Zoller, private communication.

[15] L. K .T hom sen, S. M ancini, and H .M .W iseman, Phys. Rev. A 65, 061801 (2002).

[16] J. Vanier and C .A udoin, The Quantum Physics of Atom ic Frequency Standards (IOP Publishing Ltd, 1989).

[17] B. Julsgaard, A .K ozhekin, and E .S. Polzik, N ature 413, 400 (2001).

[18] G. Santerelli, A .C lairon, S. N . Lea, and G .M .T ino, Opt. Comm. 104, 339 (1994).

[19] U. Schunemann, H .Engler, R .G rim m , M .W eiden uller, and M .Z ielenkowski, Rev. Sci. Instrum. 70, 242 (1999).

[20] H .H ansen, T .A icheler, C .H ettich, P. L odahl, A .I. Lvovsky, J. M lynek, and S. Schiller, Opt. Lett. 26, 1714 (2001).

[21] A .D andridge, J. Lightwave Technol. 3, 514 (1983).

[22] W .M . Itano, J.C .B ergquist, J. J. B ollinger, J. M .G illigan, D .J. H einzen, F .L. M oore, M .G .R aizen, and D .J. W ineland, Phys. Rev. A 47, 5 (1993).

[23] R .G rim m , M .W eiden uller, and Y .B .O vchinnikov, Adv. in Atom ., M ol. & Opt. Phys. 42, 95 (2000).

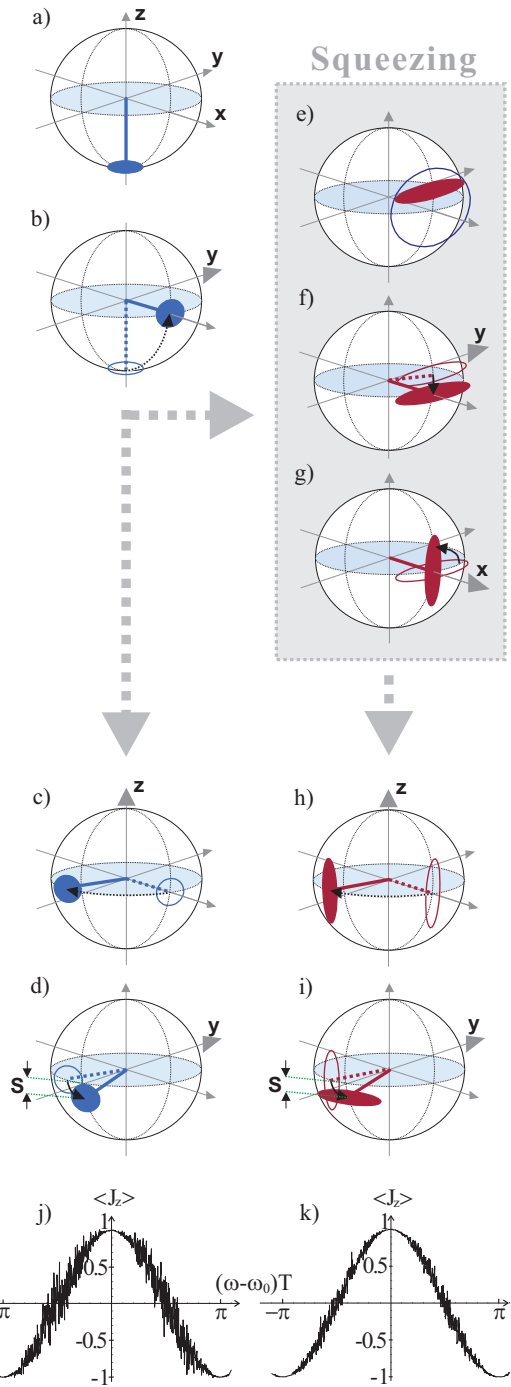


Figure 1: The Bloch-Sphere scheme for the state preparation (a,b) QND measurement (e,f,g) and the Ramsey spectroscopy for a coherent state (c,d) and a spin squeezed state (h,i), with the corresponding simulations of the noise on the Ramsey fringe, (j) and (k) respectively.

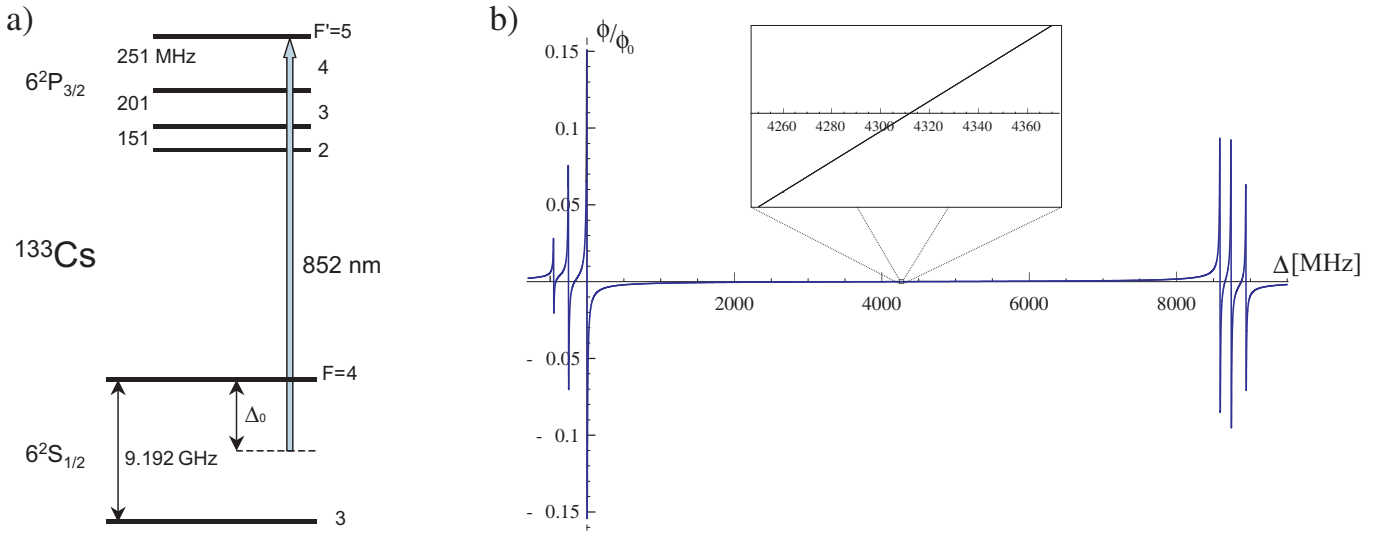


Figure 2: a) Diagram of the Cs hyperfine levels included in the D_2 line. b) Theoretically evaluated phase shift of the probe as a function of the detuning Δ from the $6S_{1/2}(F=4) \rightarrow 6P_{3/2}(F'=5)$ transition.

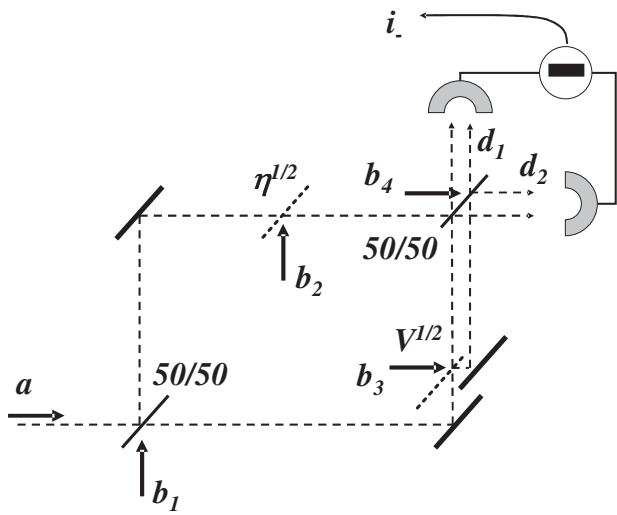


Figure 3: The Mach-Zehnder interferometer with loss sources and associated input fields indicated. The atoms are considered to be in the upper arm.

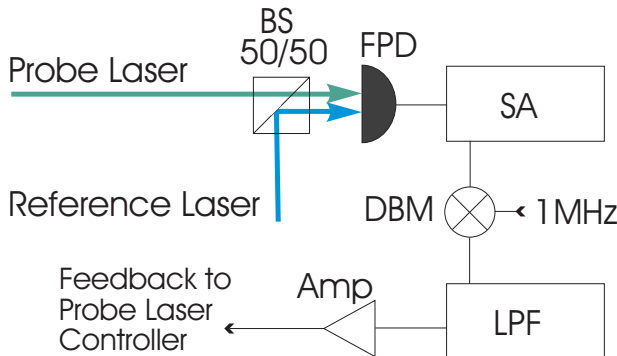


Figure 4: Experimental setup employed to lock the probe beam. The elements included in the sketch are: BS - 50/50 beam splitter; FPD - fast photodetector; SA - spectrum analyser; DBM - double balanced mixer; LPF - low pass filter; Amp - amplifier.

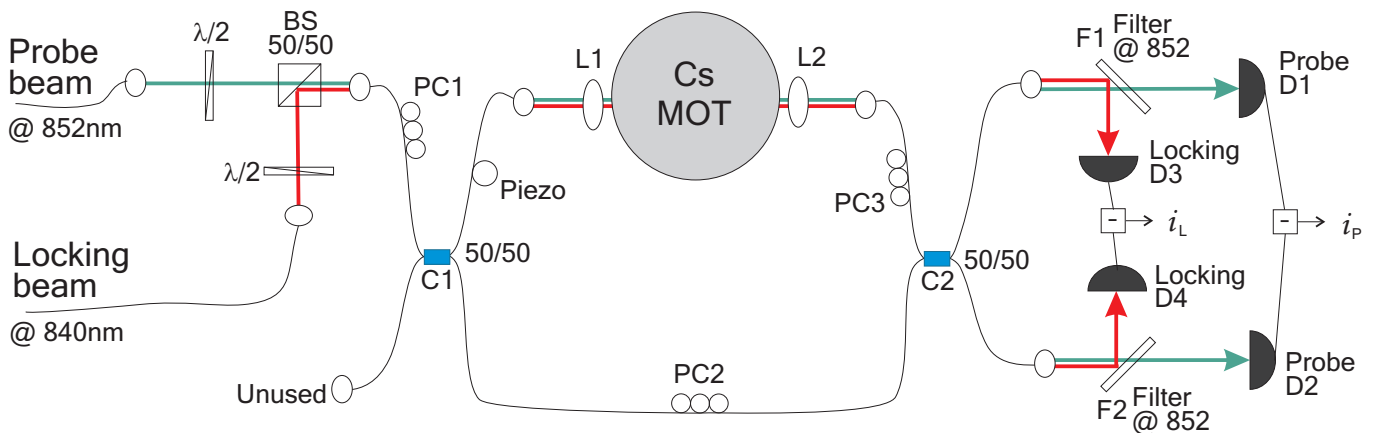


Figure 5: Sketch of the setup of the interferometer with following elements: BS - 50/50 beam splitter; C1 & C2 - 50/50 fiber couplers; PC1, PC2 & PC3 - fiber polarization controllers; L1 & L2 - achromatic lenses; F1 & F2 - interference filters transmitting @ 852 nm; D1 & D2 - Hamamatsu low noise, high gain photodiodes; D3 & D4 - photodetectors; and several half wave plates =2 and collimating lenses for fiber coupling. i_L is the locking signal, whereas $i_P = i_1 - i_2$ is the probe signal.

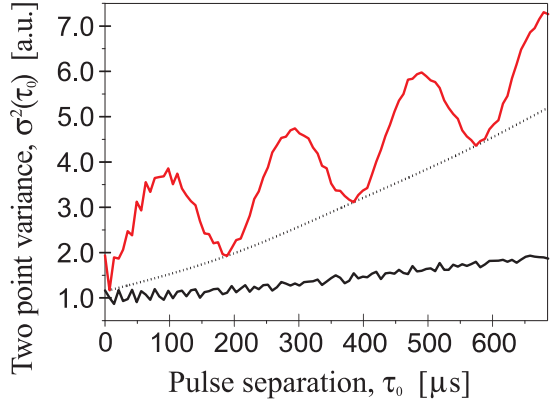


Figure 6: The two point variance extracted from measurements done with pulse separation $\tau_0 = 20$ s. Lower trace: Interferometer in white light position with probe laser locked and the variance increases on larger time scales due to the 50 Hz line noise. Upper trace: Interferometer out of white light position with probe laser frequency modulated at 50 kHz, which is directly reflected in the variance by a 200 s oscillation period. Additional phase noise from the laser raises the level of the noise in a () with respect to the lower trace, because the laser is not phase locked and the interferometer is not in the white light position.

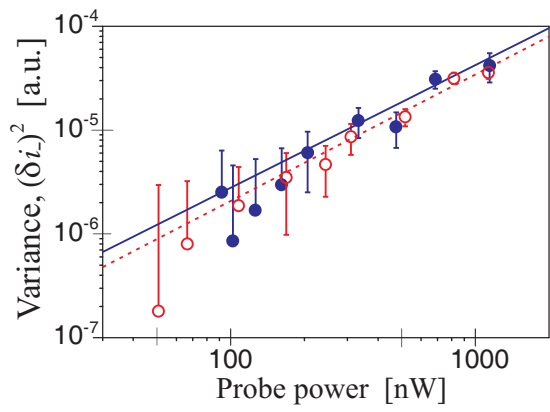


Figure 7: Noise in the amplitude x () and phase y () quadratures of the probe light. Fits to the data in log-log scale give slopes of 1.2 ± 0.2 (---) for the amplitude and 1.2 ± 0.4 (| {}) for the phase quadrature.

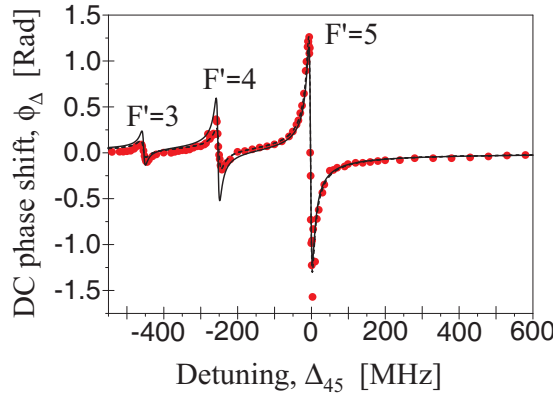


Figure 8: DC phase shift due to dispersion by the atom cloud with t (|) to Eq. (3). A closer t (---) is obtained by letting the line strengths be independent, and thus not given only by the value of the 6J-sym bals.

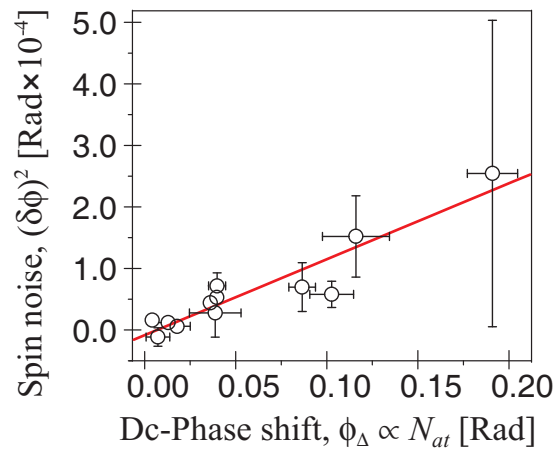


Figure 9: Phase noise induced in the probe light from the interaction with cold atoms. The DC phase shift is used as a measure for the number of atoms.